Improvement of wear and corrosion resistance of ferrous alloys by post-nitrocarburizing treatments

R. Sola, R. Giovanardi, P. Veronesi, G. Poli
Department of Materials and Environmental Engineering, University of Modena and Reggio Emilia, Italy

ABSTRACT

Gas nitrocarburizing and post-oxidation treatments were performed on 42CrMo4 and 20MnCr5 steels, G30 and GS600 cast irons, to improve wear and corrosion resistance. In both materials the thickness of the compounds layer, mainly composed by ε- and γ'- phase, resulted about 15-20 μm and the measured diffusion layer was about 150 μm thick. A subsequent oxidizing step, followed by impregnation with a two different lubricating oils was performed in order to further enhance corrosion resistance. Wear resistance against alumina was measured using a ball-on-disk tribometer and the corrosion characteristics of the samples were studied using salt spray test in accordance with ASTM B117. Experimental results show that the nitrocarburizing treatment improves significantly the wear resistance of the steels but not the wear resistance of the studied cast irons. The steels present almost the same tribological behaviour, ascribable to the formation of similar compounds, while cast irons present different wear resistance due to their chemical composition and the graphite morphology. The application of nitrocarburizing alone does not significantly improve corrosion resistance and it may even promote localized corrosion. The subsequent post-oxidation step leads to a slight decrease of the corrosion rate, because it partially seals the porous nitrocarburized layer. The final oil impregnation step resulted much more effective in further decreasing the corrosion rate and this final treatment in some cases improves also the wear resistance.

RIASSUNTO

I trattamenti di nitrocarburazione gassosa e di post-ossidazione sono stati eseguiti sugli acciai 20MnCr5 e 42CrMo4 e sulle ghise GS600 e G30 allo scopo di migliorarne resistenza a usura e le proprietà a corrosione. Dopo il trattamento di nitrocarburazione in tutti i materiali si forma uno strato di composti costituito dai nitrocarburi ε e γ', di spessore 15-20 μm, sovrastante lo strato di diffusione spesso circa 150 μm. I successivi trattamenti di ossidazione e ossidazione seguita da impregnazione in olio sono stati eseguiti per migliorare ulteriormente la resistenza a corrosione. Per la valutazione della resistenza a usura sono stati eseguiti test tribologici con un tribometro in configurazione ball-on-disk e test in nebbia salina, in accordo con la normativa ASTM B117, per la resistenza a corrosione. I risultati sperimentali mostrano che il trattamento di nitrocarburazione migliora notevolmente la resistenza a usura degli acciai ma non delle ghise studiate. Gli acciai mostrano lo stesso comportamento a usura, riconducile alla formazione di composti superficiali simili, le ghise presentano proprietà tribologiche molto differenti in funzione della morfologia superficiale. La nitrocarburazione non migliora in modo decisivo la resistenza a corrosione del materiale e promuove la corrosione localizzata. Un miglioramento delle proprietà a corrosione si ottiene con il trattamento di post-ossidazione, ma è con l'impregnazione finale che si raggiunge la massima resistenza a corrosione, accanto ad un ulteriore miglioramento alla resistenza a usura.

INTRODUCTION

Nitrocarburizing treatments have been developed for many years in order to improve wear and fatigue resistance [1,2]. Ferritic nitrocarburizing is a thermo-chemical process that diffuses nitrogen and carbon into the surface of ferrous materials at temperature completely within the ferrite phase field, in practice below the Fe-N eutectoid temperature. The result of this treatment can be subdivided into a compound layer, consisting predominantly of ε and/or γ' (Fe_4N) phases, which is responsible for the good wear resistance and high surface hardness, and in a diffusion zone, where N and C are dissolved interstitially in the ferritic matrix, thus leading to an improvement of fatigue strength when compared to an untreated material. In comparison with other technologies, nitrocarburizing is characterised by lower treatment temperature and shorter treatment time, a high degree of shape and dimensional stability, and process safety and reproducibility [3].

Present research in the field of surface treatments is attempting to develop new solutions in order to improve simultaneously mechanical and tribological properties, as well as corrosion resistance. For instance, it's possible to generate a duplex hardened layer by producing an oxide film of Fe_3O_4 on the top of compound layer after nitrocarburizing [4]. The duplex layer presents improved surface properties such as wear resistance, adhesion and self-lubrication [5]. Moreover, the presence of the oxide film leads to a significant improvement of the corrosion resistance of iron-based materials [6]. The residual open porosity of the oxidised layer [7], presenting a plurality of small pores, has no detrimental effects on corrosion resistance, since it could favour the retention of lubricant fluids, which could further increase wear resistance[8].

Aim of this study is to characterize and quantify the influence of each step of the treatment (nitrocarburizing, post-oxidation, oil impregnation) on the mechanical and tribological properties, as well as on corrosion resistance, of two steels (20MnCr5, 42CrMo4) and two cast irons (G30 and GS600).

MATERIALS AND METHODS

As substrate materials, 20MnCr5 case hardening steel, 42CrMo4 structural steel, G30 lamellar grey cast iron and GS600 spheroidal cast iron were used in the experimental studies. To verify the chemical composition of the steel a simultaneous quantometer ARL 3580 and a glow discharge optical emission spectroscopy (LECO GDS-750) were used. The resulting chemical compositions are given in the Table I.

Table 1. Chemical compositions of the four materials

	C	Si	S	P	Mn	Ni	Cr	Mo	V	Al	Mg	Cu	Fe
20MnCr5	0.21	0.25	0.02	0.02	1.31	0.08	1.20	0.02	0.01	0.02	-	-	Bal.
42CrMo4	0.43	0.19	0.03	0.03	0.75	0.09	0.97	0.18	0.09	0.020		-	Bal.
G30	3.25	1.85	0.11	0.08	0.38	0.07	0.28	0.01	0.02		-	1.03	Bal.
GS600	3.50	1.88	0.01	0.01	0.15	0.03	0.02	0.00	0.01		0.03	0.13	Bal.

Samples for gaseous nitrocarburizing were prepared in shape of discs 8 mm thick cut from a bright rod (40 mm in diameter). A 13 mm diameter central and coaxial hole was drilled in each disk to facilitate suspension in the nitrocarburizing furnace. The samples geometry and dimension is reported in Figure 1. The surface of the disks was ground on silicon carbide paper, with a final finish grid on 2000 grade paper. The disks were cleaned and degreased prior to nitrocarburizing.

The specimens were fixed onto a stainless steel tube which is held in the nitrocarburizing furnace. This allowed the workpiece to be loaded at the beginning of the furnace, slid into the pre-heated hot zone and finally quenched into a liquid
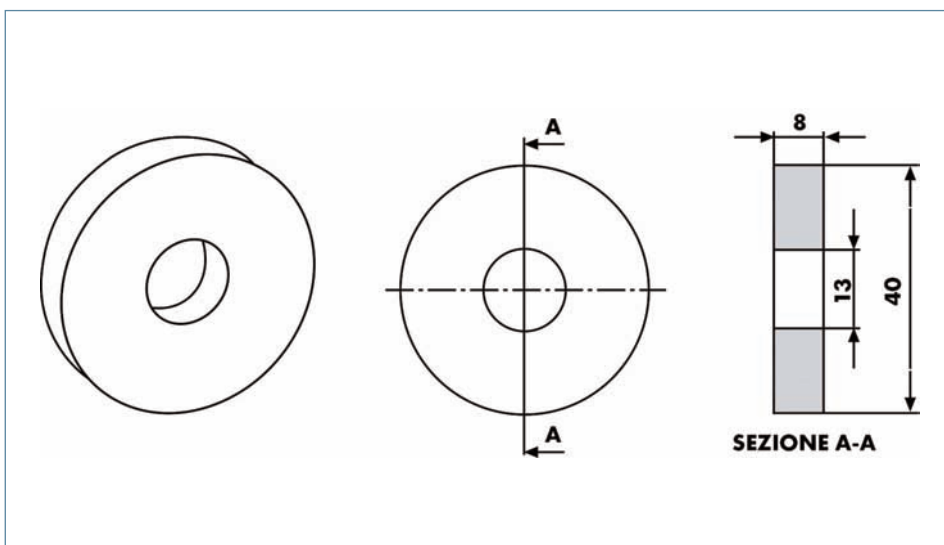

Fig. 1: samples geometry and dimension.

medium. The nitrocarburizing atmosphere consisted of a mixture of N_2, CH_4 and NH_3 injected for nitrocarburizing and of N_2, CH_4, NH_3 and N_2O in case of nitrocarburizing followed by post-oxidation. Compositional control of the furnace atmosphere is achieved by means of volume flow control. After the post-oxidation, when the samples were cooled, a further treatment step consisted of the impregnation in two different lubricating oils, dipping the samples, one at the time, for two minutes in the oils. Those oils, produced and commercialized by Houghton, act as protective and antirust films over the sample. The oils present different physical and chemical properties: RUST VETO TB oil is water based, while RUST VETO 377 oil is solvent based. Oil viscosity measurements were performed under isothermal conditions at 25°C using a Searle System

Control Rate Haake VT550 (Haake Technik GmbH, Vreden, Germany), equipped with a coaxial cylinder-measuring sensor. The measures were performed using a constant shear rate of 200 s-1.

The phases resulting from the treatments were identified by X-Ray diffraction, using $CoK\alpha$ radiation in a Philips PW 3710 diffractometer.

The treatments considered in this research are:

1. one step treatment, gaseous nitrocarburizing (samples indicated by "_NC"),

2. two steps treatment nitrocarburizing + post-oxidation (samples indicated by "_NC+O"),

3. three steps treatments nitrocarburizing + post-oxidation + impregnation in RUST VETO TB oil, water based (samples indicated by "_oil TB")

4. nitrocarburizing + post-oxidation + impregnation in RUST VETO 377 oil, solvent based (samples indicated by "_oil 377")

The samples nitrocarburized were treated at 570°C for 8 h in a gas mixture composed by N_2, NH_3 and CH_4. The post-oxidized sample were obtained from post-oxidation process at 560°C for 8 h in a N_2, NH_3, CH_4 gas mixture, followed by 1.5 h at 560°C in a N_2, CH_4, NH_3, and N_2O gas mixture.

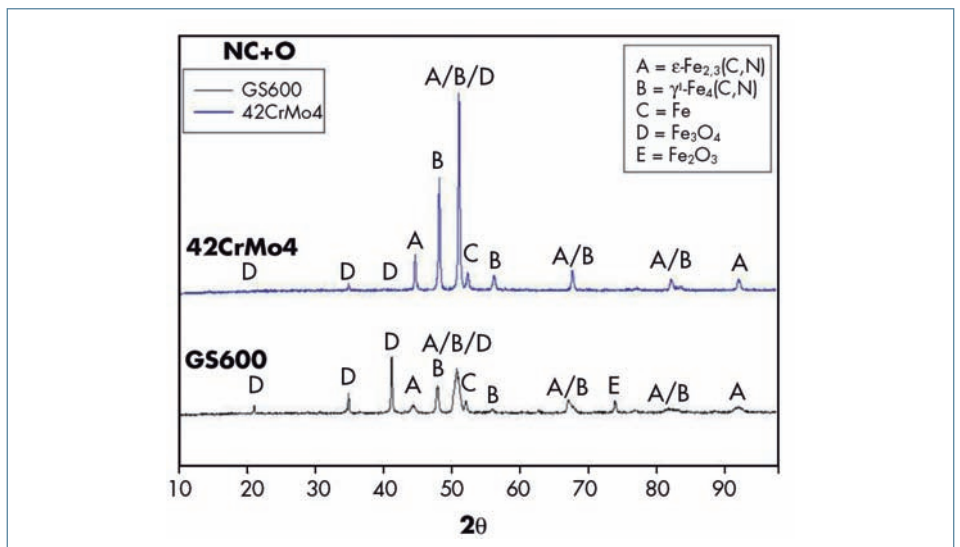The microstructures of the compounds and

Fig. 2: X-Ray diffraction pattern of 42CrMo4 NC and GS600 NC.

diffusion layers, resulting from the thermo-chemical treatments were observed on cross-sectioned samples at a Leica CTR 4000 optical microscope after polishing and etching using a 3% Nital solution. For a more detailed analysis of the structure, a Philips XL-30 scanning electron microscope (SEM), equipped with an Oxford INCA 350 energy-dispersive X-ray spectrometer (EDS), was used. Wear track morphology after tribological test was observed using SEM and optical stereomicroscope.

Vickers microhardness tests were performed using a 4.9N load on a Wolpert 401/402MVD micro-hardness tester. Tests are performed before and after each treatments and they were used to determine the microhardness profile from

cross-sectioned samples. According to UNI 10931:2001 the effective hardening depth value was determined by measuring the distance from the surface of the nitrocarburized layer to the point of the sample cross section where the hardness is 100 Vickers hardness units more than the substrate hardness. The total hardening depth value was measured as the distance from the external surface at which the Vickers hardness number of the material becomes constant and equal to the one of the substrate. Measured superficial microhardness and effective and total hardening depth of the samples are reported in Table II .

Wear rate was measured using a CSM High Temperature ball-on-disk Tribometer in

Table 2. measured superficial microhardness and effective and total hardening depth

Material	Treatment	HV0.5	Effective hardening depth [mm]	Total hardening depth [mm]
20MnCr5	Untreated	242 ± 2		
	Nitrocarburizing	790 ± 3	0.21 ± 0.01	0.28 ± 0.01
	Nitrocarburizing + post-oxidation	700 ± 3	0.30 ± 0.01	0.39 ± 0.01
42CrMo4	Untreated	298 ± 2		
	Nitrocarburizing	705 ± 3	0.22 ± 0.01	0.42 ± 0.01
	Nitrocarburizing + post-oxidation	710 ± 3	0.35 ± 0.01	0.49 ± 0.01
G30	Untreated	195 ± 2		
	Nitrocarburizing	580 ± 8	0.09 ± 0.07	0.22 ± 0.05
	Nitrocarburizing + post-oxidation	530 ± 5	0.14 ± 0.08	0.24 ± 0.08
GS600	Untreated	218 ± 2		
	Nitrocarburizing	520 ± 7	0.16 ± 0.08	0.32 ± 0.06
	Nitrocarburizing + post-oxidation	515 ± 5	0.17 ± 0.08	0.32 ± 0.05

dry sliding condition, under 5 N load and at sliding speed of 0.2 m/s for a distance of 1000 m. During test, the sample (disk) rotates against a stationary Al_2O_3 ball of 6 mm in diameter and a load cell measures the tangential force acting on the ball. Alumina was chosen as counterpart in order to have preferential wear of the disk, rather than of the ball. Wear rate was then determined measuring the wear track section using a CSM Conscan optical profilometer and calculating the volume losses of both disk (sample) and counterpart.

Corrosion test was performed using salt spray test in accordance with ASTM B117. The solution used for salt spray was NaCl 5wt% The salt spray is conducted continuously, the test temperature is maintained at 35°C ±2%, and the humidity at 94 ±4%. During testing visual inspections of the samples surface were performed every 24h, continuously, for an overall duration of 120 hours.

Specific conductance measurements on oil TB, oil 377 and saline solution used for the salt spay fog test (NaCl 5% in weight) were performed using an Analytical Control Model 120 conductimeter equipped with conductimetric cell (platinum electrodes).

RESULTS AND DISCUSSION

MICROSCOPY, X-RAY DIFFRACTION AND MICROHARDNESS

X-ray diffraction shows that, both in the steels and cast irons, after the nitrocarburizing treatment, the compounds zone is biphasic and constituted by ε-Fe_{2-3}(N,C) and γ'-Fe_4(N,C). 20MnCr5 XRD pattern is very similar to the 42CrMo4 one, and this occurs also in case of the two cast-iron samples. Figure 3 shows a representative XRD pattern of a steel, 42CrMo4, and of a cast iron, GS600. In
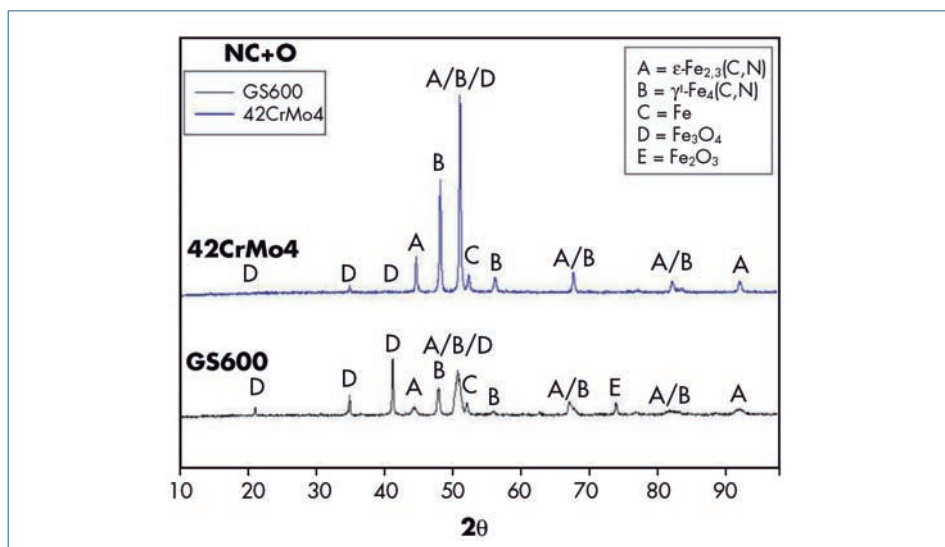

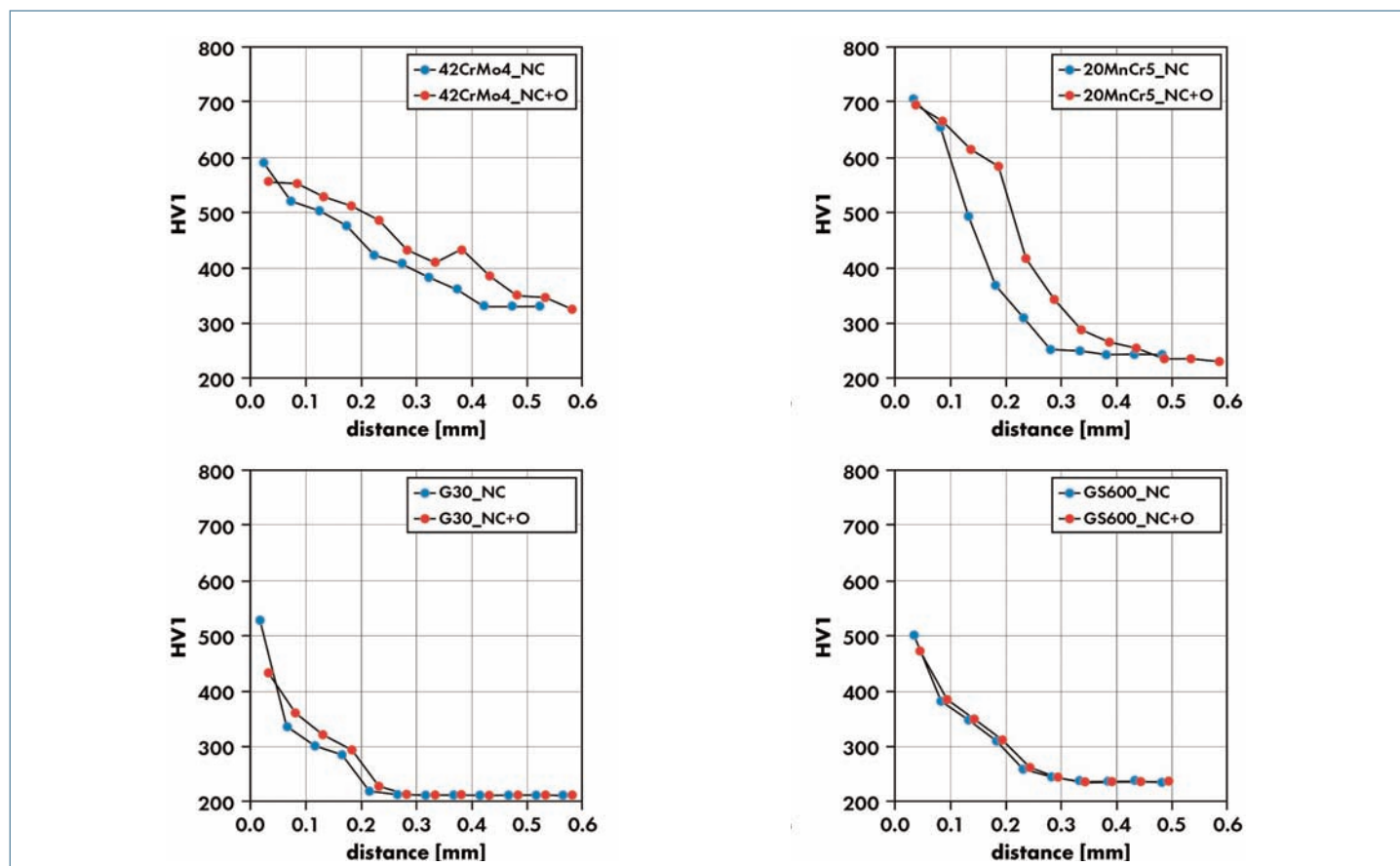Fig. 3: X-Ray diffraction pattern of 42CrMo4 NC+O and GS600 NC+O.

Fig. 4: microhardness profile of the four materials NC and NC+O.

Figure 4 is visible the XRD pattern of the post-oxidized samples, which confirms that this treatment forms, over the compounds zone, magnetite (Fe_3O_4).

The microhardness profile, reported in Figure 5, shows that the highest hardness is measured near the surface and it progressively decreases until it reaches the substrate hardness. According to UNI 10931:2001, from the microhardness profile it is possible to determinate the effective and total hardening depth, reported in Table II. In the experimental conditions applied, the effective and total hardening depth of steels resulted higher, as well as their surface hardness.

Comparing the two steels it is visible that they have a different behaviour: 20MnCr5 reaches the highest microhardness value, and also the highest increment of microhardness with respect to the bulk material; 42CrMo4 exhibits the highest effective and total hardening depth. The two cast irons present a smaller and less uniform total and effective hardening depth with respect to the steels, probably due to the blocking effect of the graphite to the nitrogen and carbon diffusion [9]. The microhardness profiles and the results of Table II show that the post-oxidation treatment tends to slightly increase the total and effective hardening depth. This could be ascribed to the prolonged exposure of the post-oxidised samples to high temperature, which favours deeper
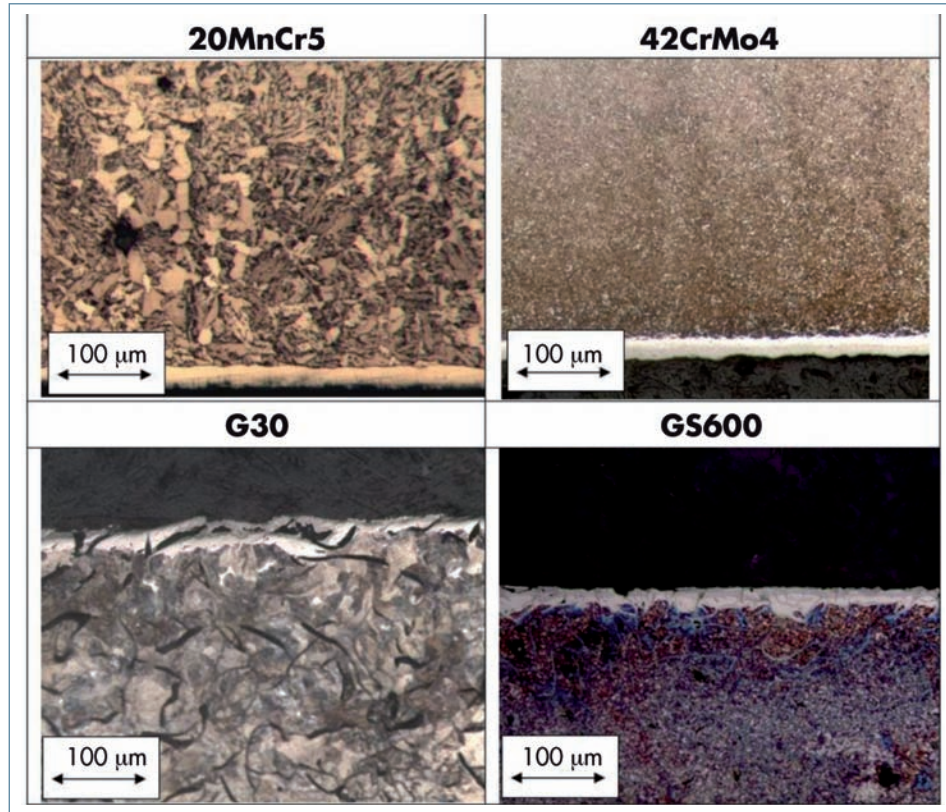

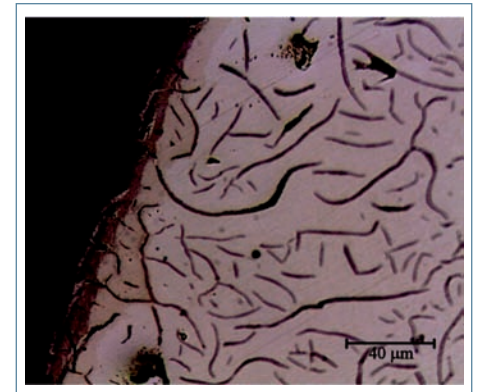Fig. 5: microhardness profile of the four materials NC and NC+O.

Fig. 6: optical micrograph of the G30 cast iron in which is visible that the thickness of the compound layer is altered by the graphite.
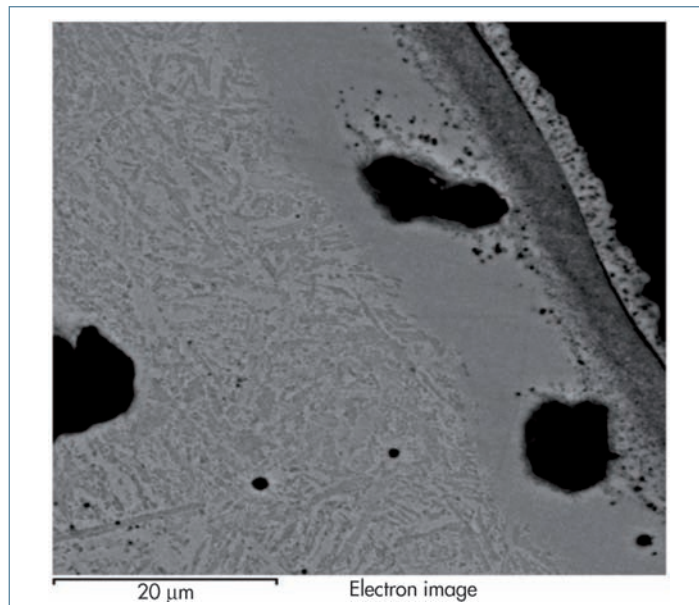

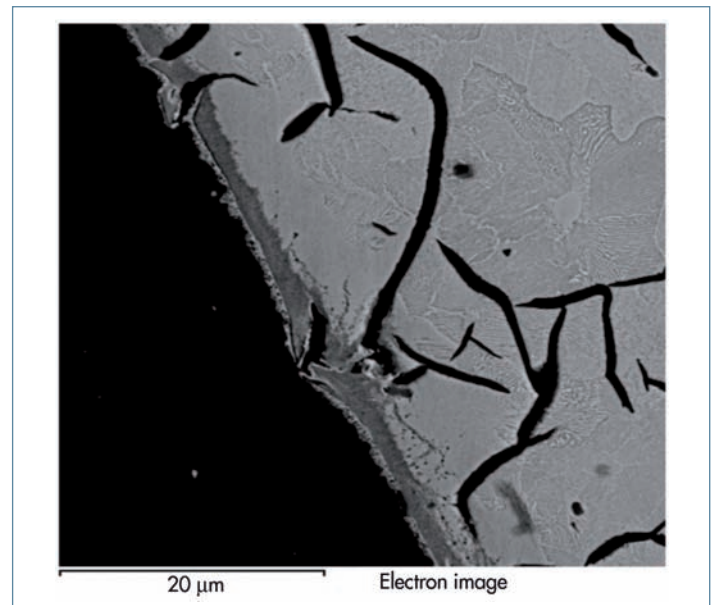Fig. 7: SEM-BSE micrograph of the GS600 cast iron NC

Fig. 8: SEM_BSE micrograph of the G30 cast iron NC

nitrogen and carbon diffusion inside the material [10].

Optical microscope analysis shows that, as expected, after nitrocarburizing both cast irons and steels present essentially the same core microstructure: ferritic and pearlitic for the 20MnCr5, primarily martensitic for the 42CrMo4, predominantly pearlitic for the G30 and martensitic with large amounts of not transformed austenite. Micrographs in Figure 6 show that in all the investigated materials nitrocarburizing induces the formation of a superficial compounds layer composed of the carbonitrides ε-$Fe_{2-3}(N,C)$, in the outer part, and γ'-$Fe_4(N,C)$, occurring predominantly in the region of the layer adjacent to the layer-matrix interface, as confirmed by XRD analysis. Below such compounds layer, the diffusion layer is present, hardened due to the precipitation of the carbonitrides along the grain boundary.

In the two steels the thickness of the compounds layer is almost constant, while in the cast irons it presents a variable thickness.   In the steels the compounds layer is well-adherent to the substrate, on the contrary of what happens in case of cast irons, probably because the graphite presence alters the diffusion of the nitrogen and carbon, as shown in Figure 7. As a matter of fact, the graphite lamellae create a kind of "boundary" between the carbon-enriched surface layers (darker regions of Figure 7, with arrows indicating the graphite limiting diffusion) and the inner parts of the steel. Moreover, the graphite morphology affects also adhesion, since, for a given C%, the spheroidical shapes are the ones which minimize surface to volume ratio. This implies that graphite flakes will tend to create a larger amount of "boundaries", able to emerge to the surface, while graphite spheroids will be less likely to emerge at the surface. This is expected to affect adhesion since no carbonitrides, acting as bonding phase, can form in correspondence of the graphite emerging at the surface. Figures 8 and 9 demonstrate the different behavior of the two cast irons according to the graphite morphology, showing that while many graphite flakes are present in the compounds layer, a much lower quantity is found in case of the spheroidal graphite cast iron.

In all the investigated materials, the post-oxidation treatment leads to the formation of an oxidized layer about 2 μm thick, over the compound zone. This treatment is useful to increase the corrosion resistance of the material because it partially fills the microporosity originated as a consequence of the nitrocarburizing.

TRIBOLOGICAL ANALYSIS

The ball-on-disk configuration allows to acquire real time information of the tribo-system, like friction, sample (steels and cast irons) wear rate and static partner (Al_2O_3 ball) wear rate.

Regarding *friction*, the tests results are reported in Figure 10 for steels and in Figure 11 for the cast irons, where the data are grouped according to the material type, varying the treatment performed.

Focusing on steels (Figure 10), it is possible to notice that in the 20MnCr5 nitrocarburizing tends to increase the friction coefficient value with respect to the untreated material. This can be mainly ascribed to the increment of the surface roughness after the treatment (measured R^1_a of untreated material is 0.57 μm, R_a of the nitrocarburized material is 1.33 μm). In fact, at the beginning of the test, when the Al_2O_3 ball slides against the rough surface, the friction coefficient in high, but at the end of the test, when the surface roughness is smoothed out by wear of the two tribo-elements, the friction coefficient is much lower. The post-oxidation, compared to nitrocarburizing, induces a reduction of friction, because of a lower surface roughness (R_a of post-oxidized sample is 1.03) and due to the lubricating effect of the oxide [10, 11]. In the applied testing conditions, the effect of oil impregnation is marginal because impregnated samples present a trend close to the post-oxidized materials one, with a slight increase of friction coefficient. The oil-impregnated 42CrMo4 exhibits a behaviour similar to 20MnCr5, but in this case the TB oil
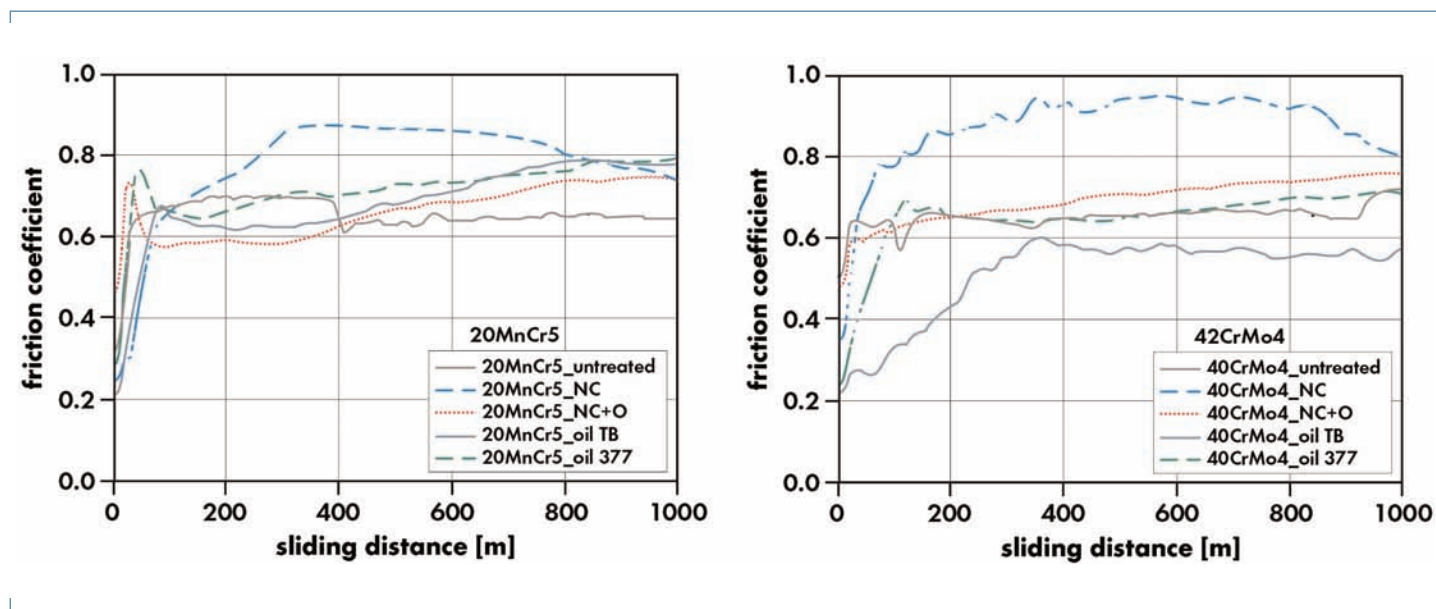

Fig. 9: friction vs sliding distance of 42CrMo4 and 20MnCr5 steels.

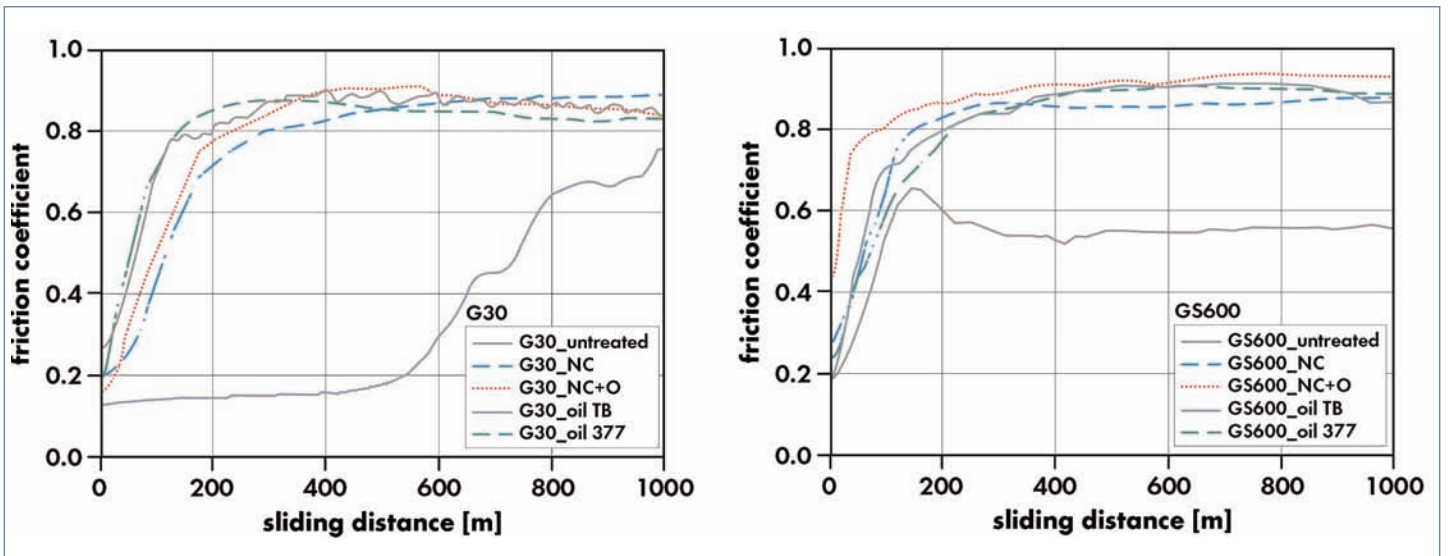[1] The Ra measurement is performed using a mechanical profilometer, SA6200

Fig. 10: friction vs sliding distance of G30 and GS600 cast irons.

contributes to maintain the friction coefficient low, especially at the beginning of the sliding. This is probably due to an initial higher availability of oil in the open porosity of the sample, which is then progressively removed as sliding proceeds. As a matter of fact, after 1000 meters sliding, the friction of the couple becomes closer and closer to the values measured for the remaining samples.

In the G30 cast iron samples (Figure 11), it is possible to notice that the untreated, nitrocarburized, post-oxidized and 377 oil impregnated exhibit all almost the same friction coefficient curve, while the TB oil impregnation results particularly efficient in maintaining a low friction coefficient up to 600 m sliding distance. Again, a possible explanation lies in the initial higher availability of oil in the open porosity of the sample. After 1000 metres sliding, all the friction values result similar, indicating that the TB-oil improvement is transient. A completely different behaviour is found in the GS600 cast iron: the untreated sample presents a lower friction coefficient throughout the whole test, while the
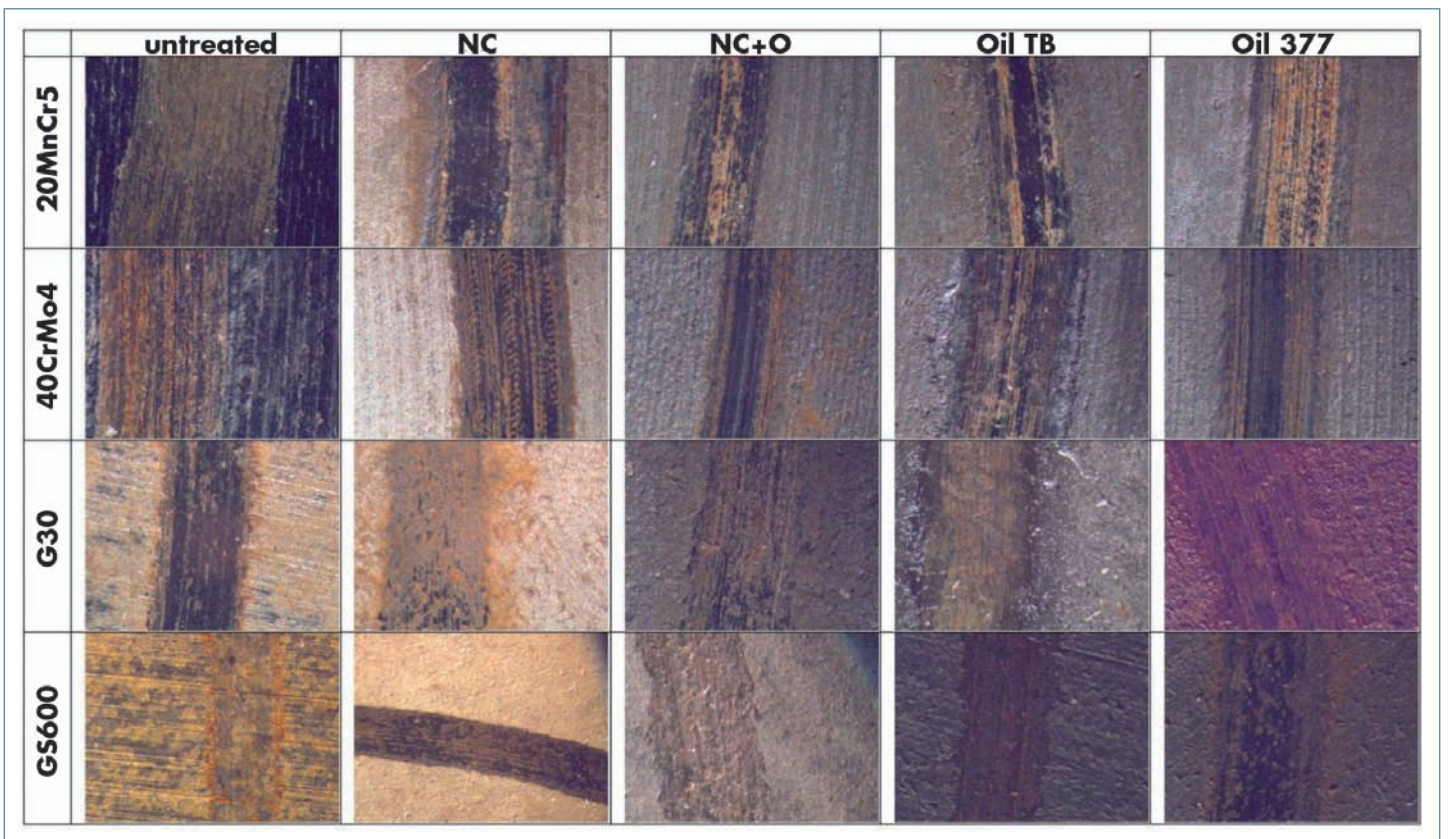

Fig. 11: optical micrographs of the wear track.

remaining samples have a similar behaviour and a higher friction coefficient value. This behaviour can be explained considering the lubricating effect of graphite and the favourable graphite morphology (spheroids), as discussed in details later. Graphite is dispersed in the whole sample mass, on the contrary of oil, which resides in the surface layer; thus, as wear proceeds, oil availability is progressively depleted, while graphite is continuously supplied at the sliding interface.

Instead, a general explanation of the measured friction values results obtained in case of impregnated samples is more difficult, because of the great variability induced by the impregnation treatment (manual immersion). However, as a general trend, the chemical and physical properties of the oils could be responsible for the better performance of the TB one: the RUST VETO TB oil is water-based, very viscous (228.0 mPa s) and it has a boiling point over 200°C, while the RUST VETO 377 oil contains 70% weight of hydrocarbonic solvent, presenting a relatively low viscosity (4.5 mPa s) and it has a boiling point close to 40°C.

Thus, during the sliding tests, at the ball-disc interface, the temperature is likely to exceed the 35°C [12], which causes the 377 oil to start degrading, making its lubricant performances decrease. The main effect of TB is to increment the sliding

distance during which the friction remains at low and constant value before raising at the level of the not impregnated samples.

Analyzing the calculated *sample wear rate*, summarised in Table III, it can be noticed that, for a given treatment, each material presents similar wear rates, probably because the treatments tend to form the same superficial compounds.

In case of steels, all the treatments induce an exceptional reduction of the sample wear rate with respect to the untreated material. The NC samples, among the treated samples, present one of the highest sample wear rate, which is slightly reduced by post-oxidation, while oil impregnation does not seem to lead to major improvements; on the contrary, the use of 377 oil causes a moderate increase of wear rate. A possible explanation of this behaviour is that, during the tribological test, locally, the temperature exceeds 35°C and the hydrocarbonic solvent evaporates, leaving a residue that forms, together with the wear debris (oxides and hard nitrocarburised particles), a viscous abrasive paste that, remaining inside the wear track, contributes to accelerate the material wear by a three body mechanism.

In case of cast irons, the untreated cast irons wear rate is lower than untreated steels, due to the presence of graphite that acts as solid lubricant. Analyzing the G30 wear rates, it can be noticed that nitrocarburization and post-oxidation

increase the sample wear rate with respect to the untreated G30. The NC samples present the highest value of sample wear rate, while the post-oxidation induces a decrease of sample wear rate. A possible explanation of the lower wear rate of the untreated samples can be the lack of graphite at the sliding interface in case of treated samples: the lubricating action of graphite results hindered by the presence of the compounds layer, which limit the availability of graphite at the sample surface. Moreover due to the localised lack of adhesion between substrate and compounds layer, during sliding hard and abrasive debris can detach and remain between the sliding couple. In case of G30 cast iron, this can be also favoured by the morphology of graphite flakes (that cause an high stress concentration) [9].

The untreated GS600 cast iron exhibits an optimum wear resistance, better than G30 one. All the treatment cause a decrease of wear resistance, probably because they inhibit the lubricant effect of the graphite and increment the abrasive component in the wear mechanisms. This fact does not happen in case of steels because the superficial treated layer are well adherent to the substrate and they create a smaller amount of hard debris, than in case of cast irons. The better performance of GS600 cast iron compared to G30 one can also be explained considering that in GS600 the graphite morphology is spheroidal and thus induces a
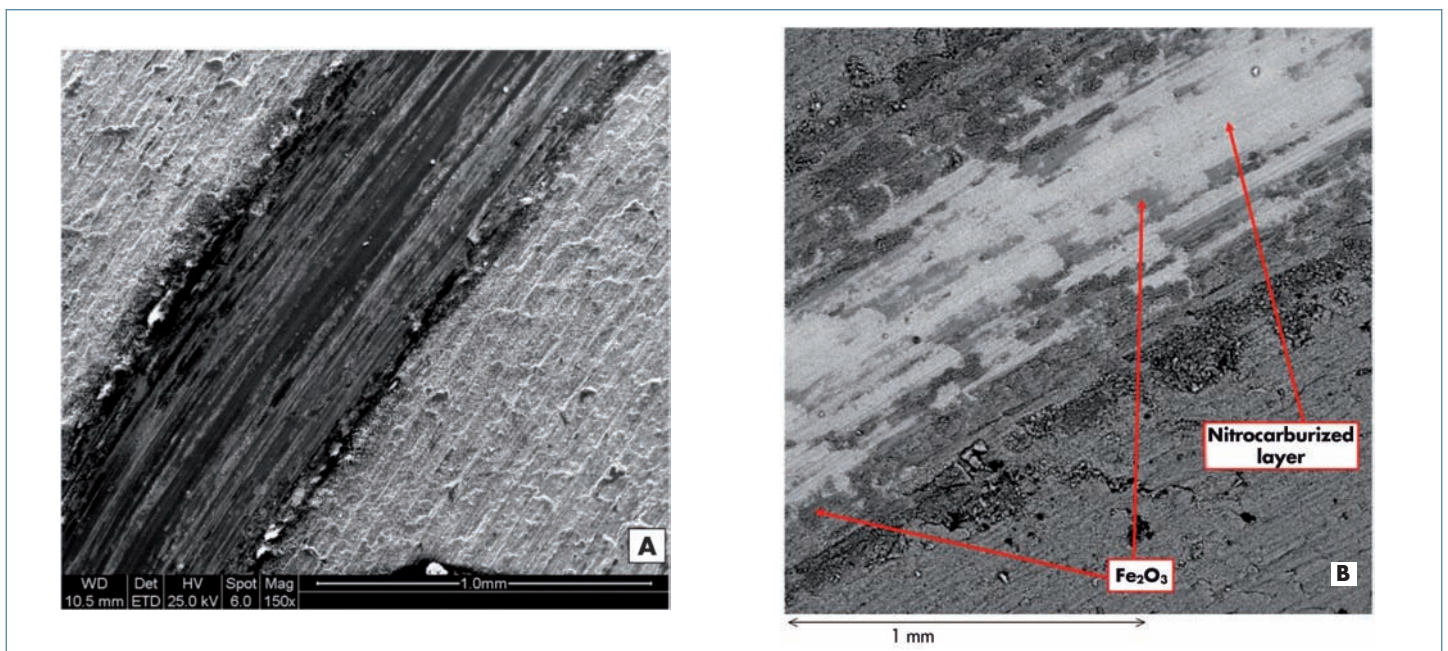

Fig. 12: A: SEM-SE micrograph of 42CrMo4 NC wear track - B: SEM_BSE micrograph of 42CrMo4 NC wear track.

lower stress concentration [13].

Figure 12 shows the optical micrographs of the wear tracks, where the presence of reddish Fe_2O_3 iron oxide compounds is evident (iron oxide deriving from post-oxidation is magnetite, dark coloured). Thus, considering also the measured wear rates, it can be inferred that under these wear conditions, the wear mechanism is mild-oxidational.

It's also clearly visible that the traces present deep furrows, probably because the harder Al_2O_3 pin crushes the softer top layers, generating hard debris (oxides and nitrocarbides). These debris, remaining inside the wear tracks, due to load applied, don't roll away, but tend to remain in the contact region between the two tribo-elements. SEM-EDS analysis confirmed that both for steels and cast irons the predominant wear mechanism is mild-oxidational, as shown in Figures 13A and B, which are referred, as an example, to the wear behaviour of 42CrMo4_NC. In the centre of the track it is present the original steel (light grey), emerged due to the local removal of the compounds layer. The nitrocarburized layer remains visible at the side of the track (dark grey). Near the track are present some debris of Fe_2O_3 (darker regions), to confirm that the wear mechanism is mild-oxidational.

Figure 14 A and B and Figure 15 show the inside of the wear track in case of cast iron. It can be seen that in the wear track there is

Table 3. Sample wear rate, Al_2O_3 pin, load 5N, 0.2 m/s

	20MnCr5 x10-5 [mm3/Nm]	42CrMo4 x10-5 [mm3/Nm]	G30 x10-5 [mm3/Nm]	GS600 x10-5 [mm3/Nm]
untreated	75.9 ± 4.7	22.1 ± 5.5	5.2 ± 0.2	0.9 ± 0.1
NC	4.8 ± 0.6	4.3 ± 0.1	8.5 ± 0.4	3.6 ± 0.8
NC+O	3.7 ± 0.3	1.8 ± 0.1	6.6 ± 0.9	2.5 ± 0.5
Oil TB	4.4 ± 0.5	1.7 ± 0.1	2.7 ± 0.3	3.1 ± 1.0
Oil 377	5.1 ± 0.7	5.3 ± 0.2	4.1 ± 0.9	4.3 ± 1.0

abundance of iron oxide (upper spectrum) originated during sliding against the alumina pin. This oxide tends to deposit where graphite from lamellas has been removed. This tendency of the wear products (iron oxide, but also hard debris) to deposit in the cavities originally occupied by graphite can explain the reason why the treatments lead to an overall decrease of wear resistance of the cast irons, as well as to an increase of friction, particularly evident in case of GS600 samples.

CORROSION – SALT-SPRAY TEST (FOG)

The improvement of corrosion resistance due to postoxidation and oil impregnation treatments was evaluated using the salt-spray (fog) test, conducted according to ASTM B117 and ISO 9227: as prescribed by the standards a visual inspection of the samples was performed every 24h, with the aim to detect the presence of corrosion products and of characteristic corrosion

morphologies on the surface of the samples. Results from visual inspections shows that all the investigated materials, subjected to the same thermochemical treatment, exhibit almost the same behavior. Figure 16 shows the aspect of the samples of 20MnCr5 steel before the salt-spray test (0h) and after 48h exposure time.

After 48h the untreated (TQ) samples are completely covered of corrosion products (red rust, ferrous oxides); these oxides are clearly not protective, as they are porous, spongy and not well adherent to the substrate. A slight corrosion resistance improvement is given by nitrocarburizing, which results further improved in case of post-oxidation treatment, since the corrosion products could are visually detectable only in few small spots. Therefore, these treatments improve the corrosion resistance, because they promote the superficial formation of nitrocarbides and protective oxides (Fe_3O_4) that, in general, are less reactive than the
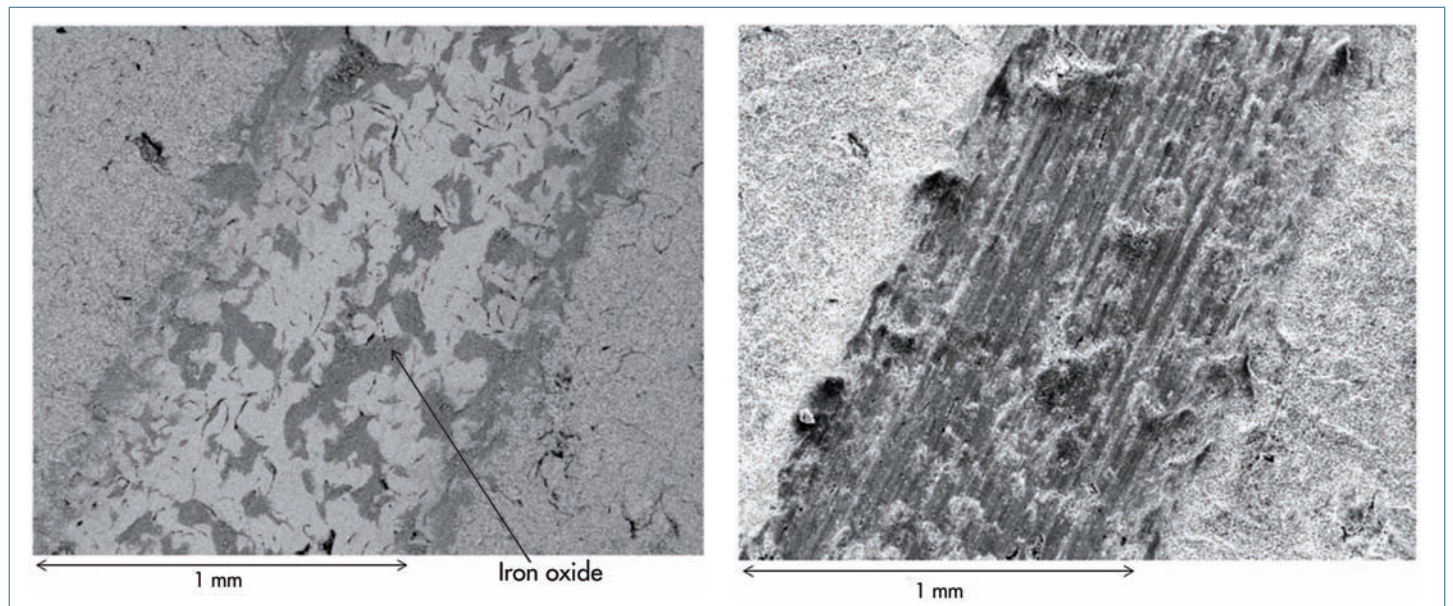

Fig. 13: A: SEM_BSE micrograph of G30 NC wear track - B: SEM-SE micrograph of G30 NC wear track.

untreated [14-22]. However, they are only partially effective in protecting the samples against corrosion in chloride media. In particular, the thin (1-2 μm) magnetite layer formed during the oxidation treatment is probably defected and not homogeneous, leaving some areas susceptible to localized corrosion.

A decisive improvement was detected in case of oil impregnation: red corrosion products are totally absent on the surface of the samples after 48h of the salt spray fog test, either in case of TB or 377 oil. The first visual evidence of corrosion products on the oil-impregnated samples was found after 120h of permanence in the saline environment: in this case only the 377 samples present small reddish areas, while the surface of TB sample remains still perfectly black.

Salt spray fog test is an industrial accepted characterization techniques, which, however, allows to evaluate the corrosion resistance only in a qualitatively way, based on the presence of noticeable corrosion products and ranking the different samples on the basis of the size of corroded areas and time of their occurrence. The obtained results confirm the quantitative findings reported in previous works form the authors [23,24], obtained using electrochemical test to evaluate corrosion potential (E_{corr}) and
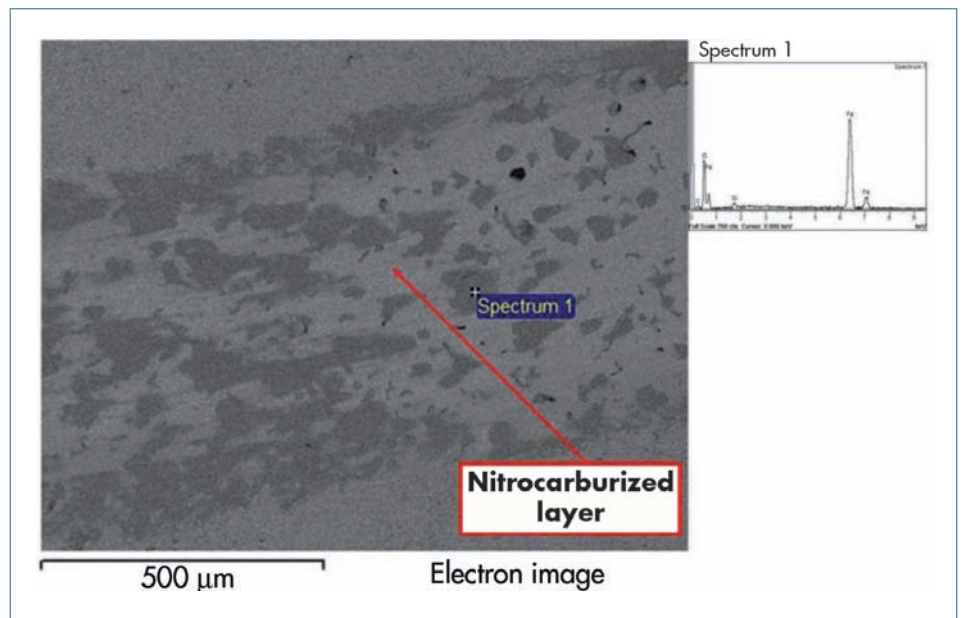

Fig. 14: SEM_BSE micrograph of G30 NC wear track.

corrosion current (i_{corr}). In this work the attention is focused on the salt spray fog results, that is a simple way to qualitatively evaluate corrosion resistance of high protective coatings/treatments [25,26].

The outstanding resistance against chloride corrosion given by oil impregnation cannot be ascribed to a simple "electric barrier" effect. The measured specific conductance of the two oils is lower than the specific conductance of the saline solution used for the test (0.61 mScm^{-1} and 0.14x10-3 mScm^{-1} for TB and 377 oils respectively, against a conductivity of 70.1 mScm^{-1} for the 5% NaCl aqueous solution). The value of TB oil is high enough to sustain high corrosion currents; moreover, the protection given by TB oil during the salt spray fog test resulted slightly higher with respect to 377 oil, while there is a difference of three order of
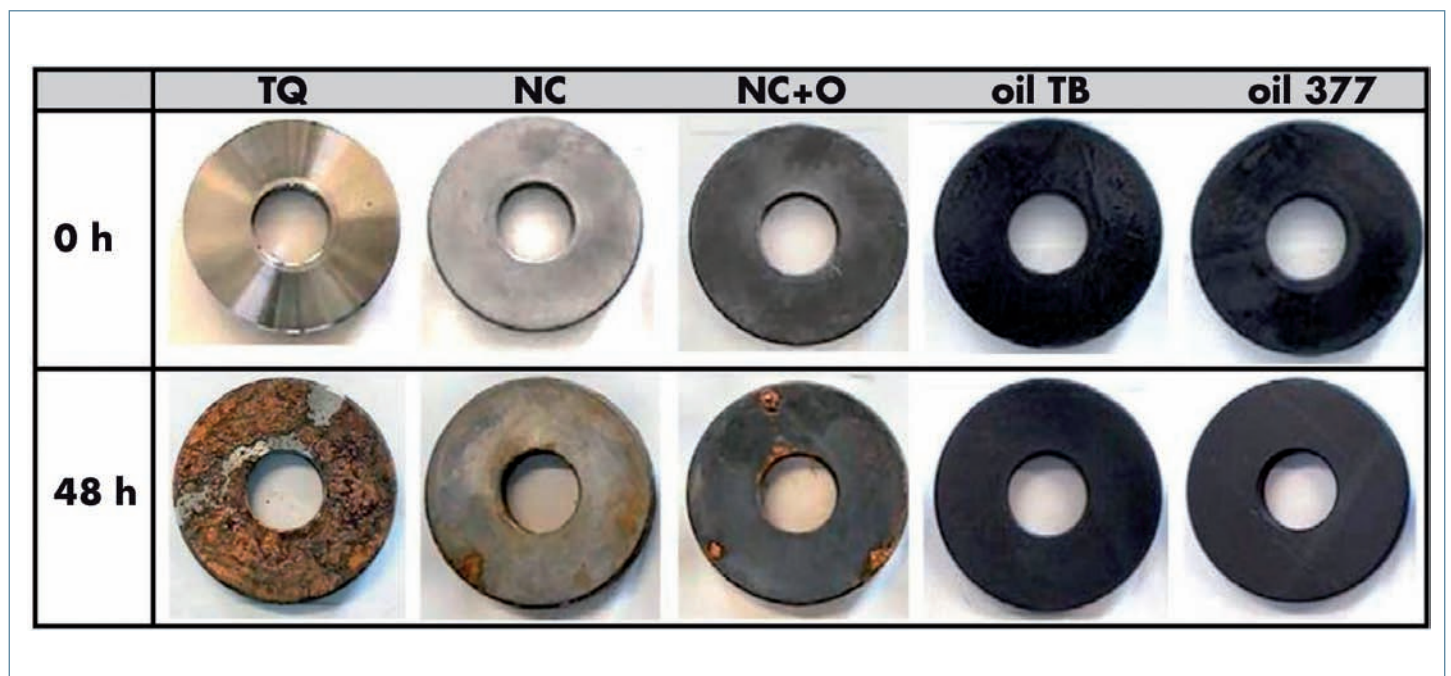

Fig. 15: photographs of 20MnCr5 steel before salt spray test (0h) and after 48h exposure time.

magnitude, in favor to 377 oil, in their specific conductivity.

The results suggest that the two oils seems to act, more properly, as corrosion inhibitors: probably they are adsorbed on the surface of the samples as a mono-molecular (or thicker) film that acts as an hydrophobic barrier avoiding the direct contact between the substrate (samples) and the electrolyte (condensed salt spray fog). This phenomena affect both cathodic and anodic reaction, and hinder the action of chloride ions (they cannot reach the metal to form soluble corrosion products)

CONCLUSION

Post-nitrocarburizing treatments, mainly post-oxidation and oil impregnation, have been performed on steels and cast irons, in order to improve their wear and corrosion resistance.

The presence of graphite in the cast irons, according also to literature results, resulted to be one of the factors affecting the homogeneity and the depth of nitrocarburizing (diffusion zone resulted 100-120 μm thick in cast irons, 150-220 μm thick in the steels), as well as the friction and the wear rate.

Nitrocarburizing and post-treatments resulted particularly effective in improving the wear resistance of steels, and in particular of 42CrMo4, whose wear rate, against Al_2O_3, is minimum. Oil impregnation, instead, had only a marginal effect on the post-oxidized steel samples wear rate.

Post-treatments on cast irons resulted less effective in increasing wear resistance and in some case led to an increase of wear rate, due to the reduced action of graphite as lubricant. Salt spray (fog) tests showed only a slight increase of corrosion resistance in case of nitrocarburizing, further improved by post-oxidation. However, the decisive improvement is given by oil impregnation in the TB oil, water base. This behaviour has been associated to the formations of a continuous oil layer which act as electrical barrier.

REFERENCES

[1] Basu, J. Dutta Majumdar, S. Ghosh Chowdhury, P.K. Ajikumar, P. Shankar, A.K. Tyagi, Baldev Raj, I. Manna, Surf. Coat. Technol., 201 (2007) 6985-6992

[2] K. Marusic, H. Otmaacic, D. Landek, F. Cajner, E. Stupnisek-Lisac, Surf. Coat. Technol. 201 (2006) 3415–3421

[3] S. Mandl, F. Scholze, H. Neumann, B. Rauschenbach, Surf. Coat. Technol., 174 –175 (2003) 1191–1195

[4] S. Barella, M. Boniardi, F. D? • Errico, A. Sironi, La Metallurg. Ital., 4 (2007) 39-45

[5] A. Alsaran, A. Çelik, C. Çelik, I. Efeoglu, Mat. Sci. Eng. A, 371 (2004) 141–148

[6] S. Hoppe, Surf. Coat. Technol., 98 (1998) 1199-1204

[7] Gui-jiang Li, Jun Wang, Qian Peng, Cong Li, Ying Wang and Bao-luo Shen, Jour. Mat. Proc. Technol., 201 (2008) 187-192

[8] M.L. Doche, V. Meynie, H. Mazille, C. Deramaix, P. Jacquot, Surf. Coat. Technol., 154 (2002) 113–123

[9] X. Nie, L. Wang, Z. C. Yao, L. Zhang, F. Cheng, Surf. Coat. Technol., 200 (2005) 1745 – 1750

[10] Eun-Kab Jeon, Ik Min Park, Insup Lee: Mat. Sci. Eng. A, 449–451 (2007) 868–871

[11] M.T. Mathew, M.M. Stack, B. Matijevic, L.A. Rocha, E. Ariza, Trib. Int., 41(2008) 141-149

[12] N. Laraqi, N. Alilat, J.M. Garcia de Maria, A. Baïri, Wear, 266 (2009) 765-770

[13] G. Nicoletto , A.Tucci , L. Esposito, Wear, 137 (1996) 38-44

[14] A.M. Abd El-Rahman, S.H. Mohamed, M.R. Ahmed, E. Richter, F. Prokert, Nucl. Instrum. Meth. Phys. Resear. B, article in press, corrected proof

[15] Insup Lee, Current Applied Physics, article in press, corrected proof

[16] K.H. Lee, K.S. Nama, P.W. Shin, D.Y. Lee, Y.S. Song, Materials Letters, 57 (2003) 2060–2065

[17] R.L.O. Basso, R.J. Candal, C.A. Figueroa, D. Wisnivesky, F. Alvarez: Surf. Coat. Technol., 203 (2009) 1293-1297

[18] M. Teimouri, M. Ahmadi, N. Pirayesh, M. Aliofkhazraei, M. Mousavi Khoee, H. Khorsand, S. Mirzamohammadi, Journ. All. Comp., article in press, corrected proof

[19] Gui-jiang Li, Jun Wang, Qian Peng, Cong Li, Ying Wang, Bao-luo Shen: Jour. Mat. Proc. Technol., 207 (2008) 187-192

[20] A. Esfahani, M. H. Sohi, J. Rassizadehghani, F. Mahboubi, Vacuum, 82 (2007) 346-351

[21] M. Karakan, A. Alsaran, A. Celik: Mat. Design, 25 (2004) 349-353

[22] A. Alsaran, H. Altun., M. Karakan, A. Celik: Surf. Coat. Technol, 176 (2004) 344-348

[23] G. Poli, R. Giovanardi, R. Sola, P. Veronesi, S. Masini, A. Zanotti: Proceeding of International Conference "Innovation in Heat Treatment for Industrial Competitivenes", Verona, Italy, 7-8 May 2008

[24] R. Sola, R. Giovanardi, P. Veronesi, G. Poli, S. Masini, A. Zanotti: proceeding of National Conference "32° Convegno Nazionale AIM", Ferrara, Italy, 24-26 September 2008.